Front. Chem. China 2009, 4(2): 121–126
DOI 10.1007/s11458-009-0026-7

RESEARCH ARTICLE

Jianhui YAN, Qiang LIU, Luxiong GUAN, Feng LIANG, Haojie GU

Photocatalytic hydrogen generation of Pt-Sr($Zr_{1-x}Y_x$)$O_{3-\delta}$-TiO_2 heterojunction under the irradiation of simulated sunlight

Abstract The Pt-Sr($Zr_{1-x}Y_x$)$O_{3-\delta}$-TiO_2 (Pt-SZYT) heterojunction photocatalysts were prepared by a photodeposition method. The composite particles were characterized by XRD, SEM, UV-Vis DRS, and PL techniques. Photocatalytic hydrogen generation in $H_2C_2O_4$ aqueous solution under the irradiation of simulated sunlight was used as a probe reaction to evaluate the photocatalytic activity of the photocatalysts. The effects of the content of Pt loading and the concentration of oxalic acid on the photocatalytic activity of the catalyst were discussed. The continuous photocatalytic activity of the Pt-SZYT and the relationship between PL intensity and hydrogen generation were also discussed. The results show that Pt-SZYT catalysts had high photocatalytic activity of hydrogen generation. The content of Pt loading and the concentration of oxalic acid have important influence on the photocatalytic hydrogen generation. The optimal loading content of platinum was 0.90 mass%. Under this condition, the average rate of photocatalytic hydrogen generation was 1.68 mmol·h^{-1} when the concentration of oxalic acid was 50 mmol·L^{-1}. The higher the photocatalytic activity, the weaker the PL intensity, which was demonstrated by the analysis of PL spectra.

Keywords heterojunction, photocatalysis, hydrogen generation, Pt, oxalic acid

1 Introduction

Recently, the rapid development of heterogeneous photocatalytic technique has provided a promising approach for semiconductor photocatalytic technique to convert solar energy to renewable hydrogen energy and solve the energy crisis. However, narrow light response spectrum and low quantum efficiency restrict the further development and application of photocatalytic technique. In order to settle these stumbling blocks, many researchers have made great efforts and received certain achievements [1–3], but there are still many problems that should be solved for the practical application of the photocatalytic technique. Our previous work [4] indicated that heterojunction composite with p-n structure is of excellent photocatalytic activity and can effectively restrict the recombination of photogenerated electrons and holes due to its special energy band structure and specific transmission for carries so as to improve quantum efficiency [5–8]. Here, Sr($Zr_{1-x}Y_x$)-$O_{3-\delta}$-TiO_2 (SZYT) heterojunction photocatalyst was modified by noble metal platinum loading, and the photocatalytic activity of the as-obtained photocatalyst was investigated for photocatalytic H_2 generation in oxalic acid aqueous solution under the irradiation of simulated sunlight.

Translated from *Acta Chimica Sinica*, 2008, 61 (in Chinese)

Jianhui YAN (✉), Qiang LIU, Luxiong GUAN, Haojie GU
Department of Chemistry and Chemical Engineering, Hunan Institute of Science and Technology, Yueyang 414000, China
E-mail: yanjh58@163.com

Jianhui YAN, Qiang LIU, Feng LIANG
School of Chemistry and Chemical Engineering, Central South University, Changsha 410083, China

2 Experiments

2.1 Photocatalysts preparation

The preparation of SZYT photocatalyst was referred to reference [4]. Here, the optimal mass ratio of the heterojunction photocatalysts (TiO_2:Sr($Zr_{1-x}Y_x$)$O_{3-\delta}$) was 70:30, which was marked as SZYT-70 and served as the photocatalyst substrate before modification.

The preparation of Pt loaded photocatalyst was referred to reference [9]. The SZYT-70 was ultrasonic dispersed in methanol solution (V_{H_2O} : V_{MeOH}= 99:1) containing chloroplatinic acid for 15 min, and after further agitation for 30 min, the system was directly irradiated with 250 W high-pressure Hg lamp in N_2 atmosphere for 10 h. The photo-reduction of chloroplatinic acid resulted in the formation of highly dispersed Pt particles deposited on the surface of SZYT-70 photocatalyst. After filtration and

wash with distilled water, the Pt loaded photocatalyst was calcined at 200°C for 2 h to remove the methanol and other impurity.

2.2 Photocatalysts characterization

The morphology of the as-prepared photocatalyst was characterized with a Japan JEOL JSM-5600LV Scan Electron Microscope (SEM). The crystal phase of the as-obtained photocatalyst was identified by powder X-ray Diffraction Method (XRD, Rigaku D/max 2550 VB^+ 18 kW) using Cu Kα radiation from 5°–85° and operating conditions of 40 kV and 300 mA with graphite as filter. The UV-Vis Diffuse Reflectance Spectrum (UV-Vis DRS) of the as-prepared photocatalysts was measured with an UV-Vis Spectrometer (UV-3101PC). The photoluminescence measurements (PL) were obtained with an LS-55 Fluorescence Spectrometer.

2.3 Photocatalytic activity testing

The photocatalytic activity of the as-prepared photocatalysts was evaluated by monitoring the amount of H_2 evolution from aqueous oxalic acid solution under simulated sunlight irradiation. The photocatalytic reaction was carried out in self-made tube-shaped quartz reactor (600 mL), including three layers connected with gas collecting devices, and water was used as the external circulation cooling and wind as the internal cooling. A 250 W xenon lamp was used as the light source (wavelength, 200–1100 nm; main wavelength, 400–700 nm; UV light $< 5\%$; without filter). Before the photocatalytic reaction, the photocatalyst was ultrasonic dispersed, and system was deaerated with nitrogen for 30 min to remove the oxygen in the system. During the photocatalytic reaction, the photocatalyst was kept in suspension state by a magnetic stirrer. After the photocatalytic reaction, the photocatalyst was centrifugal separated. The hydrogen gas product was analyzed by gas chromatography with ICD detector using a molecular sieve 13X and nitrogen as the carrier gas.

3 Results and discussion

3.1 Photocatalyst characterizations

3.1.1 Morphology analysis

The morphology of the as-prepared photocatalyst was characterized with SEM, as shown in Fig. 1. It can be seen that there exist larger aggregations in Pt loaded heterojunction. However, the surface of the catalyst particles is composed of many uniform nanoparticles to form a loose surface that provides better adsorption circumstance and photocatalytic reaction sites.

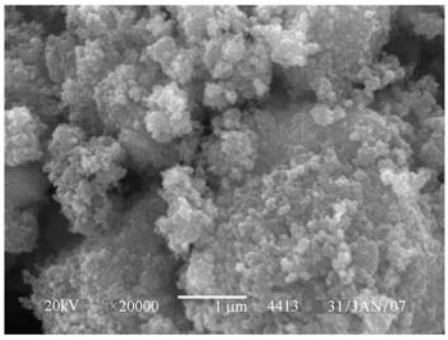

Fig. 1 SEM pattern of the as-obtained Pt-SZYT-70

3.1.2 XRD analysis

Figure 2 depicts the XRD patterns of the as-prepared photocatalysts. From the diffraction lines, it can be observed that the photocatalyst is mainly composed of anatase TiO_2 and $SrZrO_3$. There are also some rutile TiO_2 and ZrO_2 impurity that can be detected. After Pt deposition, intensity of the diffraction peaks of $SrZrO_3$ decreases to a certain extent. No diffraction peaks of Pt were observed in the XRD patterns. This is because the platinum particles were highly uniform dispersed on the surface of the photocatalyst particles, and the low content of Pt (w(Pt)= 0.90%) is under the detection limit.

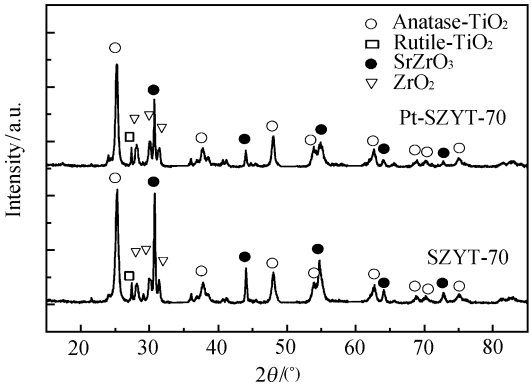

Fig. 2 XRD patterns of the as-obtained catalysts SZYT-70 and Pt-SZYT-70

3.1.3 UV-Vis DRS analysis

The UV-Vis DRS of the as-prepared Pt-SZYT-70, TiO_2, and $Sr(Zr_{1-x}Y_x)O_{3-\delta}$ are described in Fig. 3. It is clear that TiO_2 shows light absorption below 400 nm. The slight absorption of $Sr(Zr_{1-x}Y_x)O_{3-\delta}$ at long wavelength spectrum is due to the formation of defects by Y^{3+} doping [7]. After Pt loading, the heterojunction shows obvious

absorption at long wavelength spectrum, which indicates that the heterojunction can exhibit certain visible light response, and the deposition of Pt on the surface of photocatalyst particles can help to the absorption and reflection of light. Mei *et al.* [10] showed that the deposition of noble metal particles on the surface of photocatalyst particles can form a narrow metal band potential between the band gaps of the composite semiconductors, and this narrow metal band potential can act as transfer location to absorb visible light with long wavelength, enhance the visible light absorption ability, and enlarge the light response spectrum.

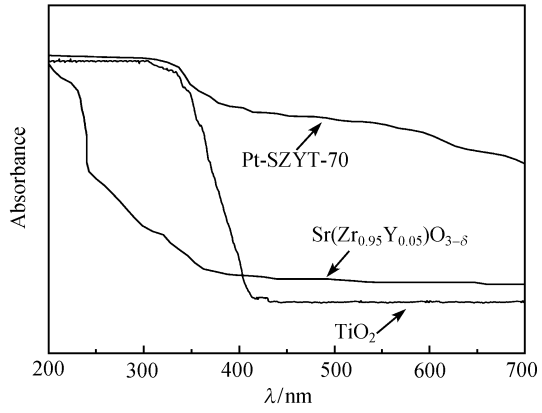

Fig. 3 Diffuse reflectance spectra of the as-obtained catalysts

3.1.4 PL analysis

PL is an effective method for researching on the electronic structure and optical properties of the semiconductor nanoparticles and for showing the information of the transfer, trap, and recombination of photo-generated carriers [11, 12]. Fig. 4 presents the PL spectra of TiO_2, SZYO, SZYT-70, and Pt-SZYT-70. The excitation wavelength is 250 nm, and the excitation and emission slits are all 5 nm.

As shown in Fig. 4, TiO_2 exhibits high PL spectrum intensity at 360–420 nm, and there are obvious peaks at 396 and 420 nm. The peak at 396 nm responds to the band gap of TiO_2 (E_g= 3.2 eV), resulting from the recombination of photo-generated holes and electrons, which directly go back from conduct band to valence band [13]. The peak at 420 nm is because that the excited electrons at higher conduct band first transit to metastable state on the conduct band and then transit to a valence band to recombine with the excited holes [14]. The PL peaks of TiO_2 are broadened, which is because the defect structure in nanoparticles can form defect energy band in band gap, and the excited electrons are first trapped by the defect energy band in the transition process and then transited to a valence band [15]. The PL peaks of SZYO are weak. This is mainly because that the band gap of $SrZrO_3$ is broad (E_g= 5.0 eV), and the energy of the excitation photons is not enough to excite the electrons from valence band to conduct band. As a result, $SrZrO_3$ only shows weak PL spectrum at 350~430 nm resulted from the defect structure. The PL spectrum of SZYT-70 shows that the coupling of TiO_2 and SZYO can reduce the PL intensity, which means that the formation of p-n heterojunction structure can help to separate the photo-generated electron and hole, so as to reduce the recombination of the photo-generated carriers [4]. Pt-SZYT-70 shows much lower PL intensity, suggesting that the deposition of Pt particles on the surface of catalyst particles further enhances the separation of photo-generated electron and hole and reduces the recombination of the photo-generated carriers.

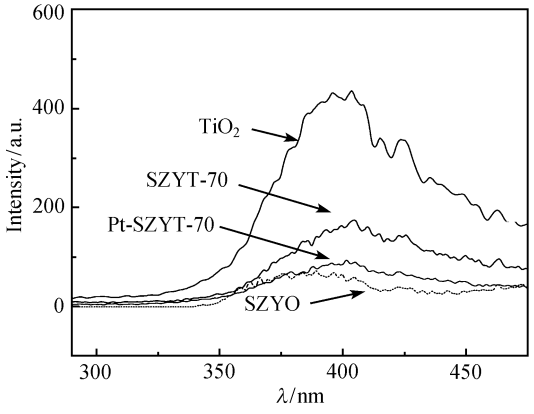

Fig. 4 PL spectra of different catalysts

3.2 Photocatalytic H_2 evolution activity

3.2.1 Effect of photocatalyst type

Figure 5 presents the effect of photocatalyst type on the H_2 evolution activity (insert is the local magnification of three similar curves). As can be seen, without oxalic acid, there is nearly no H_2 generated by adding SZYT-70 into distilled water under simulated sunlight irradiation. On the other side, without photocatalyst, there is also only trace H_2 generated from oxalic acid solution under simulated sunlight irradiation for 8 h, whereas the addition of SZYT-70 can improve the H_2 evolution rate to a certain extent, and the addition of Pt-SZYT-70 can effectively improve the H_2 evolution rate (the average rate is 1.68 mmol·h^{-1}). The loading of Pt on the surface of the photocatalyst particles can build a Schottky energy barrier, promoting the separation of photo-generated carriers. Besides, the existence of Pt can also reduce the overpotential of hydrogen on the surface of the photocatalyst particles [16]. There is almost no H_2 generated without oxalic acid

in solution, indicating that the addition of electron donor is crucial. Industrial pollutant oxalic acid is a low-cost and excellent electron donor (E_0 (CO_2/HO_2CCO_2H)= −0.49 V). Oxalic acid can reversibly combine with the photo-generated holes or surface hydroxyl and restrict the recombination of electrons and holes, so as to efficiently enhance the photocatalytic H_2 evolution efficiency.

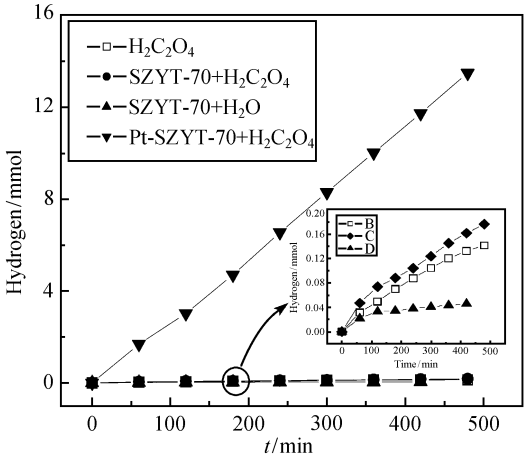

Fig. 5 Hydrogen generation at different react conditions

The photocatalytic mechanism of the Pt loaded composite photocatalyst is explored as follows: Without Pt loading, when the p-n heterojunction composite photocatalyst is irradiated, there exist surplus holes and surplus electrons on the p-type semiconductor Sr $(Zr_{1-x}Y_x)O_{3-\delta}$ and n-type semiconductor TiO_2, respectively. The photo-generated electrons and holes temporarily separate with the effect of heterojunction, but they recombine soon. Moreover, the potential between the sides of heterojunction with carriers enrichment can hinder the production of photo-generated charges. However, the loaded small Pt clusters on the TiO_2 surface act as an improvement function for the transfer of the photo-generated charges. Because the work function of Pt (Φ_m) is higher than that of TiO_2 (Φ_s), the electrons on the TiO_2 continuously transfer to the loaded Pt; meanwhile, the contact of TiO_2 and Pt can bend the energy band to create a wasting layer and form a shallow trap Schottky energy barrier for electron trapping between the interface of Pt-catalyst. Therefore, when the composite photocatalyst was irradiated by simulated sunlight, the small Pt clusters on the n-type semiconductor TiO_2 act as good trap and collector to collect the surplus electrons, which react with the absorbed H^+ to generate H_2. The Pt loading can help to the separation and transfer of photo-generated charges, effectively reduce the potential in the heterojunction, prolong the life-span of photo-generated carriers, restrict the recombination, and improve the quantum efficiency of the photocatalytic reaction.

3.2.2 Effect of Pt loading content

From the discussion above, it can be concluded that Pt loading is significant for the improvement of the H_2 evolution rate. In order to get the optimal Pt loading content, the H_2 evolution activity experiments of Pt loaded heterojunction with different Pt loading content were performed under the same conditions as mentioned above. From Table 1, it can be seen that the heterojunction shows the best H_2 evolution activity at Pt loading content w(Pt)= 0.90%, and the total H_2 evolution is 10.1 mmol after irradiated for 6 h. Meanwhile, according to the PL analysis of different Pt loading content in Fig. 6, the PL intensity of the catalyst shows the "decrease-increase-decrease" trend with the increase of Pt loading content. The change of the H_2 evolution activity of the Pt loaded catalyst is adverse as a whole to that of the PL intensity. The PL spectrum results from the recombination of the electron-hole [17–19], and the PL intensity of the catalyst reflects the recombination extent of the photo-generated carriers. Below the optimal content, the increase of Pt loading content can reduce the recombination of the photo-generated carriers exhibiting the decrease of PL intensity and increase of catalytic activity. Nevertheless, overmuch Pt particles will act as the recombination center of the photo-generated carriers; meanwhile, the light scatter caused by the overmuch Pt particles may reduce the light absorption by composite catalyst and depress the adsorption of oxalic acid on the surface of the catalyst, resulting in the decrease of the photocatalytic activity.

Table 1 Effect of Pt amount on photocatalytic H_2 generation of photocatalysts

w(Pt)/%	0.2	0.4	0.9	2.0	4.0
H_2/mmol	8.48	5.22	10.10	5.16	7.82

Note: Solution 600 mL, c_0(oxalic acid) = 50 mmol/L, m(cat) = 0. 60 g, reaction tim: t = 6 h

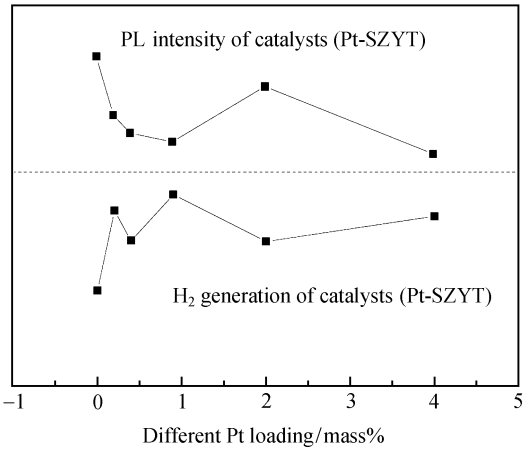

Fig. 6 The relationship between photocatalytic H_2 generation and PL intensity of the as-obtained photocatalysts

3.2.3 Effect of oxalic acid concentration

From the discussion above, it concludes that the oxalic acid concentration is also significant to the H_2 evolution activity. Therefore, the effect of oxalic acid concentration was also investigated, as illustrated in Fig. 7. Because the continuous change of the oxalic acid concentration during the reaction, the reaction time should be as short as the product can be detected so as to determine the initial reaction rate. It is clear that the H_2 evolution rate is independent of the oxalic acid concentration when c_0(oxalic acid) > 10.0 mmol·L^{-1}, whereas the H_2 evolution rate reduces with the decrease of the oxalic acid concentration when c_0(oxalic acid) < 10.0 mmol·L^{-1}. The effect of oxalic acid concentration on the H_2 evolution activity is consistent with Langmuir-type isotherm, implying that the decomposition of oxalic acid takes place in the adsorbed phase on the surface of the catalyst.

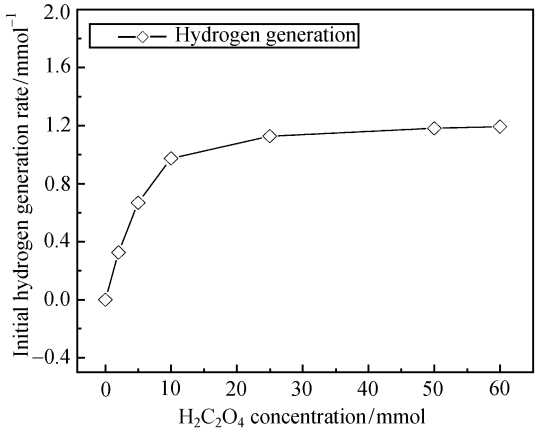

Fig. 7 Initial rate of photocatalytic H_2 generation as a function of c_0(oxalic acid) Solution 600 mL, m(0. 90%Pt-SZYT-70)= 0. 60 g , t = 30 min

3.3 Durability of the photocatalysts

In order to test the durability of the photocatalysts, w(0.90%)Pt-SZYT-70 was chosen as the representation to perform the continuous photocatalytic H_2 evolution experiment, as shown in Fig. 8. After the former run, certain amount of oxalic acid was added directly into the reaction system to recover the oxalic acid concentration to its initial value kept in the dark with agitation for 30 min, and then turned on the lamp to continue the next H_2 evolution experiment.

The results show that the H_2 evolution activity decreases a little during the continuous H_2 evolution experiment. It may be due to the rudimental product produced in the former run on the surface of the catalyst if it had not been desorbed completely before the next run. It affects the transfer of the charges and carriers on the surface of the

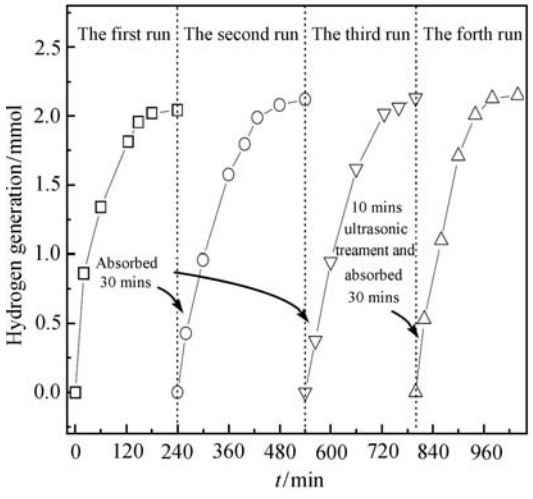

Fig. 8 Continuous photocatalytic hydrogen generation of photocatalyst under visible light irradiation Solution 600 mL, m(0. 90% Pt-SZYT-70)= 0. 60 g, c_0(oxalic acid)= 8.0 mmol·L^{-1}

catalyst, the further adsorption of the reactant, and the latter photocatalytic reaction, resulting in the decrease of the photocatalytic activity [20]. After the third run, the reactor was ultrasonicly cleaned for 10 min and then the reaction was continued by adding new oxalic acid. It can be seen that the H_2 evolution rate of the fourth run is higher than that of the second run and third run, indicating that the adsorption of catalyst on the inner wall of the reactor and the gather between the catalyst particles affect the H_2 evolution activity. Though the initial H_2 evolution rate decreases to a certain extent in the fourth run, the total amount of H_2 evolution (2.15 mmol) for 4 h is a little higher than that of the first run (2.04 mmol). It may be because the unreacted oxalic acid in the former runs can act as the electron donor in the fourth run, enhancing the total amount of H_2 evolution. The results show that the Pt loaded catalyst is a stable photocatalyst that has high catalytic performance and has a good life span.

4 Conclusion

(1) The as-obtained Pt-SZYT-70 photocatalyst shows excellent photocatalytic H_2 evolution activity in oxalic acid aqueous solution under the irradiation of simulated sunlight. The average H_2 evolution rate of w(0.90%)Pt-SZYT-70 was 1.68 mmol·h^{-1} when the mass concentration of photocatalyst and the concentration of oxalic acid were 1.0 g·L^{-1} and 50 mmol·L^{-1}, respectively.

(2) The content of Pt loading and the concentration of electron donor oxalic acid show various effects on the photocatalytic activity of the catalyst. The optimal loading content of platinum was 0.90 mass%, and the higher the photocatalytic activity, the weaker the PL intensity.

(3) The continuous photocatalytic activity experiment

indicates that the as-obtained Pt-SZYT-70 photocatalyst is of stable catalytic performance and with long life span.

Acknowledgements This work was supported financially by the National Natural Science Foundation of China (No. 20876039), the Scientific Research Foundation of Hunan Provincial Education Department of China (No. 08A026).

References

1. Wilke K, Breuer H D. Influence of transition metal doping on the physical and photocatalytic properties of titania. J Photochem Photobio A: Chem, 1999, 121(1): 49–53
2. Jiang H Q, Wang P, Xian H Z. Preparation and photocatalytic activities of low amount Yb^{3+} doped TiO_2 composite nanopowders. Acta Chim Sinica, 2006, 64(2): 145–150 (in Chinese)
3. Liu S X, Qu Z P, Han X W, Sun C L, Bao X H. Effect of silver deposition on photocatalytic activity of TiO_2. Chinese J Catal, 2004, 25(2): 133–137 (in Chinese)
4. Liu Q, Guan L X, Yan J H, Xu L. Preparation and photocatalytic property of $SrZr_{1-x}Y_xO_{3-\delta}$-$TiO_2$ composite particles. J Inor Chem, 2007, 23(2): 347–352 (in Chinese)
5. Sakthivel S, Geeissen S U, Bahnemann D W, Murugesan V, Vogelpohl A. Enhancement of photocatalytic activity by semiconductor heterojunctions: α-Fe_2O_3, WO_3 and CdS deposited on ZnO. J Photochem Photobio A: Chem, 2002, 148: 283–293
6. Bessekhouad Y, Robert D, Weber J V. Bi_2S_3/TiO_2 and CdS/TiO_2 heterojunctions as an available configuration for photocatalytic degradation of organic pollutant. J Photoch Photobio A, 2004, 163: 569–580
7. Omata T, Otsuka-Yao-Matsuo S. Photocatalytic behavior of titanium oxide-perovskite type $SrZr_{1-x}Y_xO_{3-\delta}$ composite particles. J Photochem Photobio A: Chem, 2003, 156: 243–248
8. Bessekhouad Y, Robert D, Weber J V. Photocatalytic activity of Cu_2O/TiO_2, Bi_2O_3/TiO_2 and $ZnMn_2O_4/TiO_2$ heterojunctions. Catal Today, 2005, 101: 315–321
9. Abe R, Sayama K, Arakawa H. Efficient hydrogen evolution from aqueous mixture of I^- and acetonitrile using a merocyanine dye-sensitized Pt/TiO_2 photocatalyst under visible light irradiation. Chem Phys Lett, 2002, 362: 441–444
10. Mei C S, Zhong S H. Photocatalytic synthesis of MAA from propylene and carbon dioxide over Cu/WO_3-TiO_2 catalyst. Chem J Chin Univ, 2005, 26: 1093–1097
11. Zhang W F, Zhang M S, Yin Z. Photoluminescence in anatase titanium dioxide nanocrystals. Appl Phys B, 2000, 70, 261–265
12. Li X Z, Li F B, Yang C L, Ge W K. Photocatalytic activity of WO_x-TiO_2 under visible light irradiation. J Photochem Photobiol A: Chem, 2001, 141: 209–217
13. Jing L Q, Sun X J, Cai W M, Xu Z L, Du Y G, Fu H G. The preparation and characterization of nanoparticle TiO_2/Ti films and their photocatalytic activity. J Phys Chem Solid, 2003, 64: 615–623
14. Liu L, Jiang X, Liang J H, Li Y D, Li F L. Photoluminescence of tetragonal ZrO_2 nanoparticles synthesized by severral methods. Spectro and Spectral Anal, 2005, 25: 1026–1029
15. Zhang L D, Mo C M. Luminescence in nanostructured materials. Nanostructured Materials, 1995, 6: 831–834
16. Linsebigler A L, Lu G Q, Yates J T. Photocatalysis on TiO_2 surface: principles, mechanisms and selected results. Chem Rev, 1995, 95: 735–758
17. Fujihara K, Izumi S, Ohoo T. Time-resolved photoluminescence of particulate TiO_2 photocatalysts suspended in aqueous solutions. J Photochem Photobiol A: Chem, 2000, 132: 99–104
18. Hiramoto M, Hashimoto K, Sakata T. Electron transfer and photoluminescence dynamics of CdS particles deposited on porous vycor glass. Chem Phys Lett, 1987, 133: 440–444
19. Jing L Q, Sun X J, Cai W M, Li X Q, Fu H G, Hou H G, Fan N Y. Photoluminescence of Ce doped TiO_2 Nanoparticles and their photocatalytic activity. Acta Chim Sinica, 2003, 61(8): 1241–1245 (in Chinese)
20. Jing L Q, Xu Z L, Sun X J, Shang J, Cai W M, Du Y G, Fu H G. Photocatalytic activity of ZnO and TiO_2 particles and their deactivation and regeneration. Chinese J Catal, 2003, 24(3): 175–180 (in Chinese)